Electronic Supplementary Material (ESI) for Journal of Materials Chemistry A.
This journal is © The Royal Society of Chemistry 2019

Supporting Information

Amorphous Fe/Mn Bimetal-Organic Frameworks: Outer and Inner Structural Design for Efficient Arsenic(III) Removal

*TianshuZhang,[a] Jing Wang,[a]WentaoZhang,[a]ChengyuanYang,[a] Liang Zhang,[a]WenxinZhu,[a] Jing Sun,[b]GuoliangLi,[c] Tao Li,[d]Jianlong Wang [a]**

[a.] College of Food Science and Engineering, Northwest A&F University, Yangling, 712100, Shaanxi, China. E-mail: wanglong79@yahoo.com.

[b.] Qinghai Key Laboratory of Qinghai-Tibet Plateau Biological Reources, Northwest Institute of Plateau Biology, Chinese Academy of Sciences, 810008, Qinghai, China.

[c.] Key Laboratory of Life-Organic Analysis of Shandong Province, Qufu Normal University, Qufu, 273165, Shandong, China.

[d.] Shaanxi institute for Food and Drug Control, Xi'an, 710065, Shaanxi, China.

* Corresponding authors:wanglong79@yahoo.com.

Supporting Figures

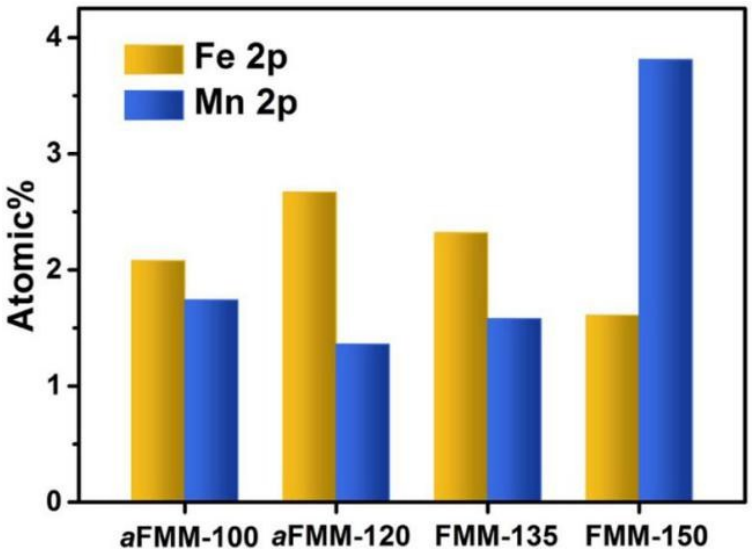

Figure S1. Distribution of the Fe and Mn contents of FMMs by using XPS in this work.

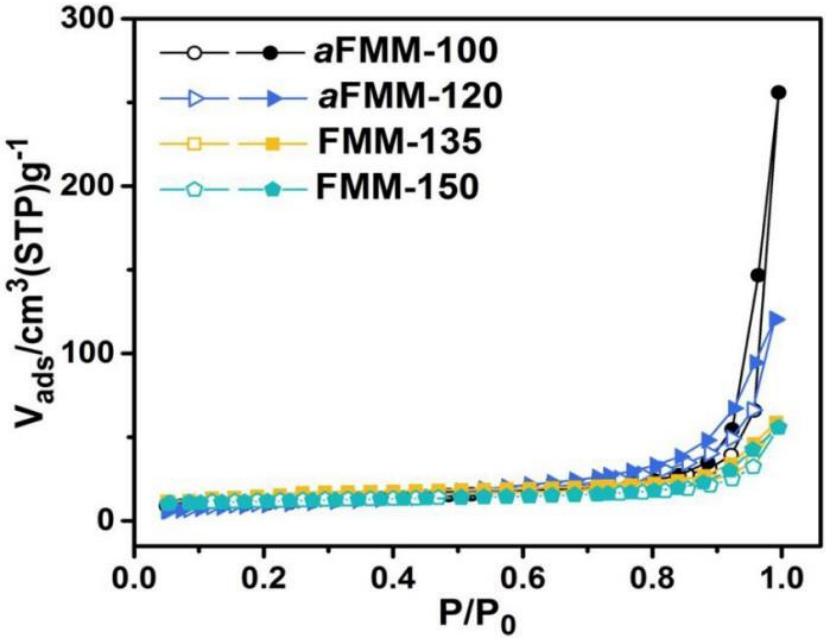

Figure S2. N_2 adsorption/desorption isotherms of aFMM-100, aFMM-120, FMM-135 and FMM-150 taken at 77 K.

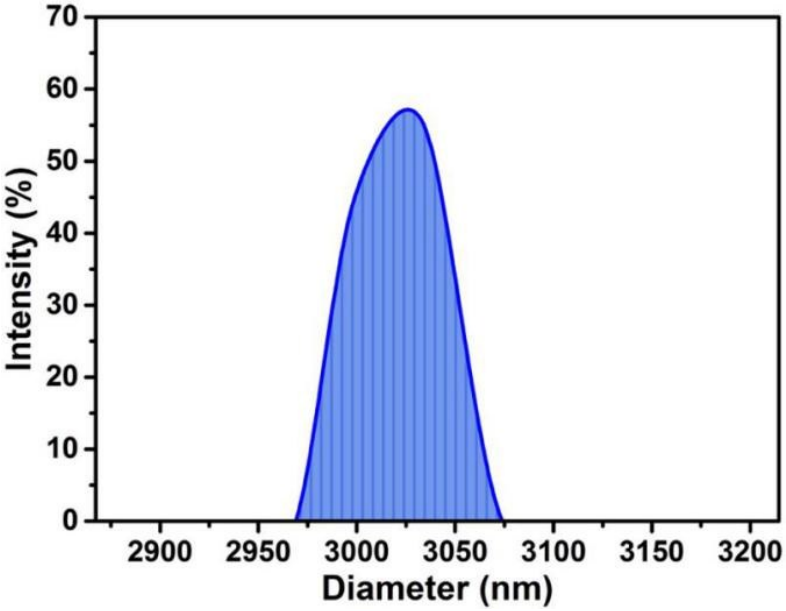

Figure S3. Size distribution of aFMM-120 in water determined by using DLS.

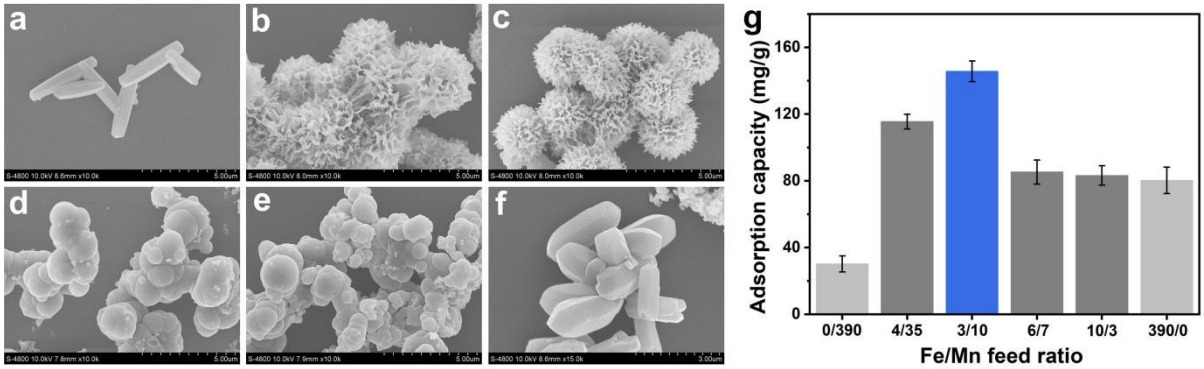

Figure S4. a-f) The SEM images of MOF-74s with increased Fe/Mn feed radios from 0/390 to 390/0. **g)** The adsorption performance of MOF-74s toward As(III) with different Fe/Mn feed radios.

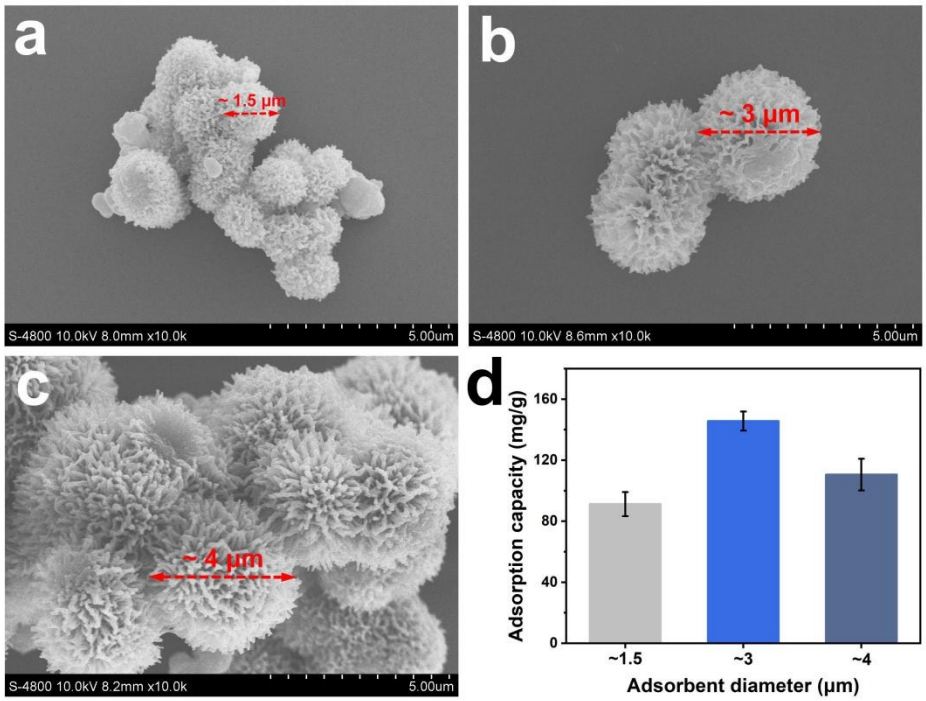

Figure S5.a-c) SEM images of aFMM-120s with different sizes of ~1.5 μm, ~3 μm and ~4 μm and **d)** the corresponding adsorption capacities toward arsenic species.

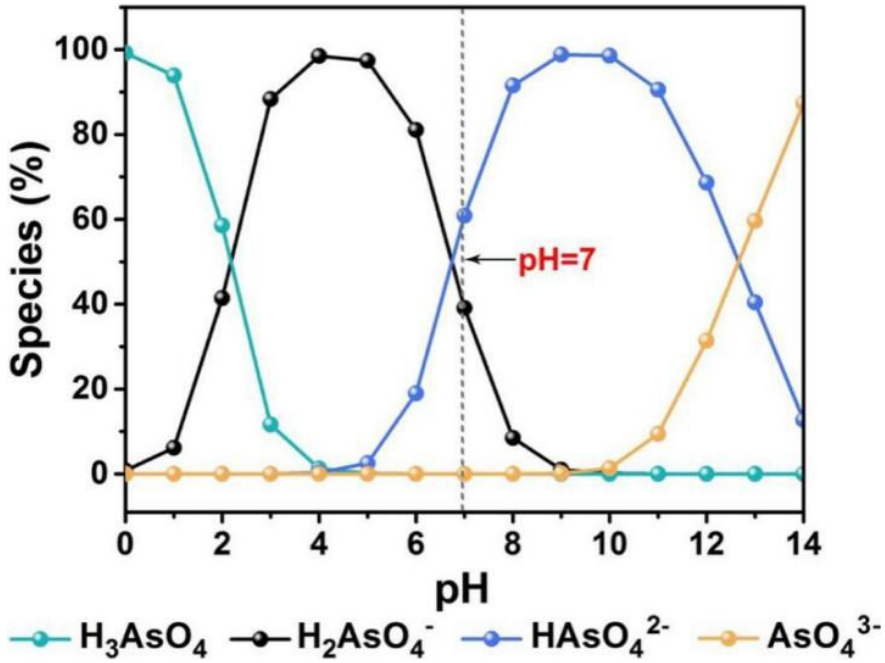

Figure S6. Different species of As(V) with changing pHs (0-14) obtained by Visual MINTEQ software programme.

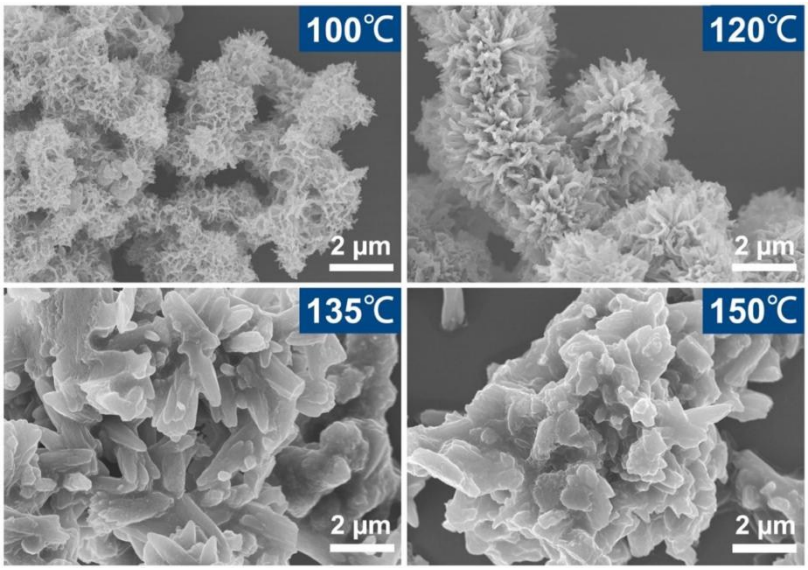

Figure S7. The photographs of aFMM-100, aFMM-120, FMM-135 and FMM-150after oxidation/adsorption of arsenic.

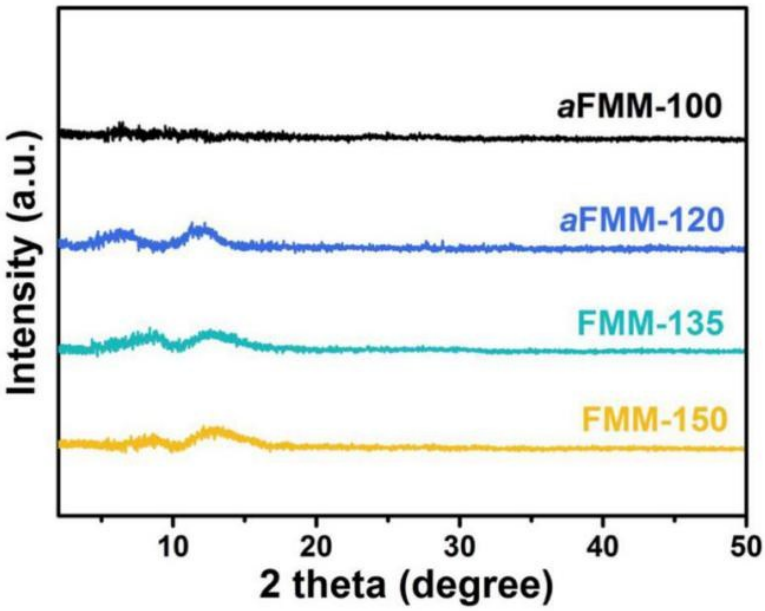

Figure S8. XRD patterns of aFMM-100, aFMM-120, FMM-135 and FMM-150after oxidation/adsorption of arsenic.

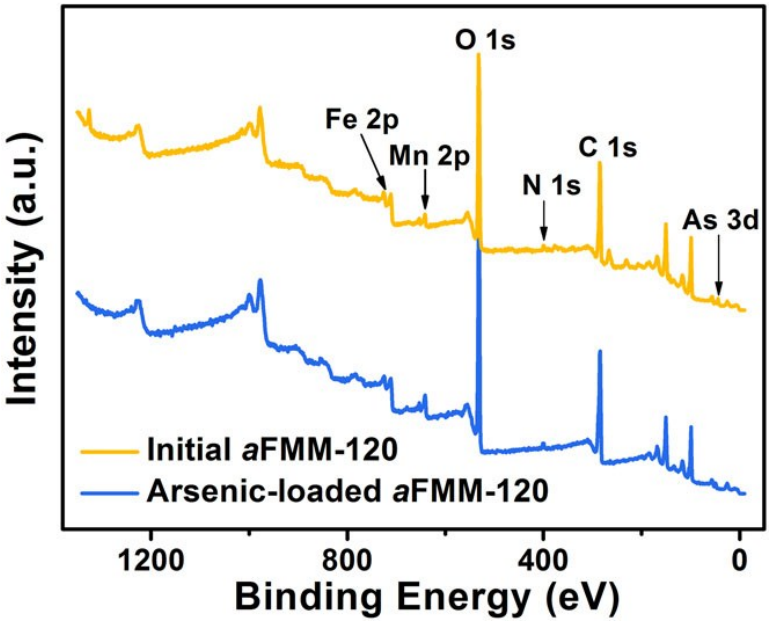

Figure S9. XPS wide scan spectrum of aFMM-120 before andafter oxidation/adsorption of arsenic.

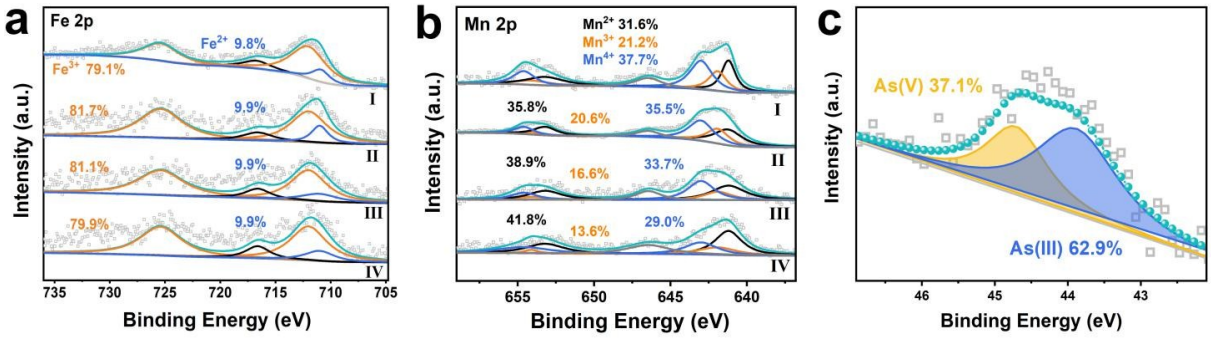

Figure S10. High resolution XPS spectra of **a)** Fe 2p and **b)** Mn 2p of regenerated aFMM-120 in four adsorption-desorption cycles from I to IV. **c)** High resolution XPS spectra of As 3d in the eluent.

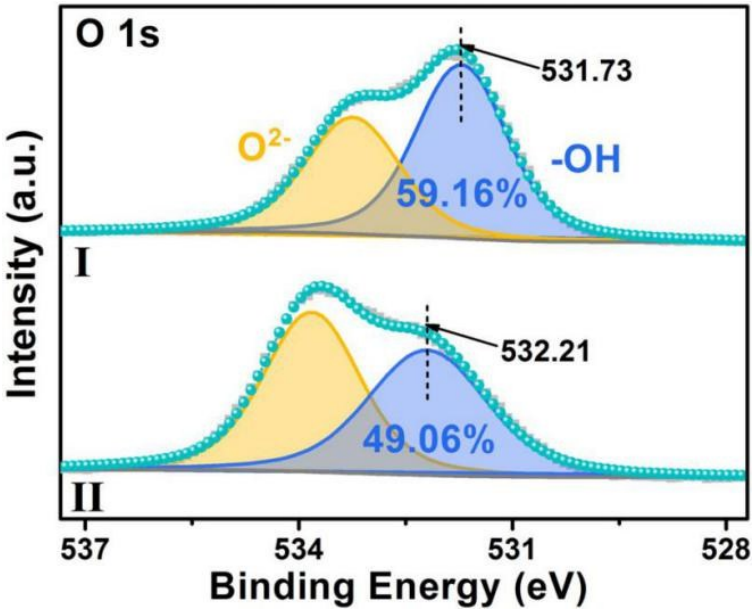

Figure S11. O 1s XPS spectra of aFMM-120 before andafter oxidation/adsorption of arsenic.

Supporting Tables

Table S1. Arsenic adsorption kinetics parameters using pseudo-second-order model on aFMM-120.

Concentration	pseudo-second-order			
(mg/L)	$q_{e,\ exp}$(mg/g)	k_2 (g/mg min)	$q_{e,\ cal}$(mg/g)	R^2
5	5.518	0.02587	5.924	0.9926
10	13.97	0.01668	14.54	0.9985
20	28.89	0.01751	29.42	0.9994
30	46.36	0.009612	46.64	0.9964
50	79.05	0.003961	81.28	0.9936

Table S2. Kinetic fitting parameters using pseudo-first order and intra-particle diffusion models of As(III) adsorption on aFMM-120.

Concentration (mg/L)	pseudo-first-order			intra-particle diffusion		
	k_1 (min^{-1})	q_e(mg/g)	R^2	k_i	C_i	R^2
5	0.1067	5.298	0.9907	0.8918	0.5918	0.9956
10	0.1549	13.24	0.9803	0.9457	7.663	0.9889
20	0.2613	27.75	0.9921	2.202	16.98	0.8246
30	0.2484	43.57	0.9745	3.213	26.75	0.2942
50	0.1957	74.86	0.9807	7.300	36.82	0.6721

Table S3. Isotherms parameters using Langmuir and Freundlich isotherm model of As(III) adsorption on aFMM-120.

Temperature (K)	$q_{max,exp}$(mg/g)	Langmuir isotherm model			Freundlich isotherm model		
		k_L	$q_{max,cal}$(mg/g)	R^2	k_F (mg/g)	n	R^2
298	138.0	0.009529	230.4	0.9592	4.374	1.433	0.9901
308	145.7	0.009077	258.4	0.9831	4.340	1.386	0.9934
318	161.6	0.01439	233.6	0.9782	7.465	1.595	0.9903

Table S4. Comparison of maximum As(III) adsorption over different adsorbent materials.

Adsorbents	Adsorption capacity to As (III) (unit: mg/g)	Equilibrium time	Reference
UIO-66	40	24 h	1
MnO_2@ZIF-8	147.28	24 h	2
$CoFe_2O_4$@MIL-100(Fe)	143.6	2 min	3
ZIF-8nps	49.49	13 h	4
Fe_3O_4@MIL-101(Cr)	121.5	24 h	5
Cubic ZIF-8	122.6	10 h	6
Leaf-shaped ZIF-8	108.1	10 h	6
Dodecahedral ZIF-8	117.5	10 h	6
Fe mesh@MIL-100(Fe)	35.2	6 h	7
Fe_3O_4@ZIF-8	100.0	4 h	8
Fe_3O_4-RGO-MnO_2	14.04	40 min	9
Fe-Mn binary oxide	100.4	16 h	10
Ce-Mn binary oxide	97.7	14 h	11
Ceria associated manganese oxide	34.89	40 min	12
Zr-Mn binary oxide	104.5	/	13
Magnetic Fe–Mn binary oxide	56.1	60 min	14
aFMM-120	161.6	70 min	this work

References

1. C. Wang, X. Liu, J. P. Chen and K. Li, *Sci. Rep.,* 2015, **5**, 16613.
2. M. Jian, H. Wang, R. Liu, J. Qu, H. Wang and X. Zhang, *Environ.Sci.:Nano,* 2016, **3**, 1186–1194.
3. J. Yang and X. Yin, *Sci. Rep.,* 2017, **7**, 40955.
4. M. Jian, B. Liu, G. Zhang, R. Liu and X. Zhang, *Colloids Surf., A,* 2015, **465**, 67–76.
5. K. Folens, K. Leus, N. R. Nicomel, M. Meledina, S. Turner, G. V. Tendeloo, G. D. Laing and P. V. D. Voort, *Eur. J. Inorg. Chem.,* 2016, 4395–4401.
6. B. Liu, M. Jian, R. Liu, J. Yao and X. Zhang, *Colloids Surf., A,*2015, **481**, 358–366.
7. D. Wang, S. E. Gilliland, X. Yi, K. Logan, D. R. Heitger, H. R. Lucas and W.-N. Wang, *Environ. Sci. Technol.,*2018, **52**, 4275−4284.
8. J.-B. Huo, L. Xu, J.-C. E. Yanga, H.-J. Cui, B. Yuan and M.-L. Fu, *Coll. Surf. A,* 2018, **539**, 59–68.
9. X. Luo, C. Wang, S. Luo, R. Dong, X. Tu and G. Zeng, *Chem. Eng. J.,* 2012,**187**, 45–52.
10. G. Zhang, J. Qu, H. Liu, R. Liu and R. Wu, *Water Res.,* 2007, **41**, 1921–1928.
11. J. Chen, J. Wang, G. Zhang, Q. Wu and D. Wang, *Chem. Eng. J.,* 2018, **334**, 1518–1526.
12. K. Gupta, S. Bhattacharya, D. Nandi, A. Dhar, A. Maity, A. Mukhopadhyay, D.J. Chattopadhyay, N.R. Ray, P. Sen and U.C. Ghosh, *J. Colloid Interf. Sci.,* 2012, **377**, 269–276.
13. G. Zhang, A. Khorshed and J. Paul Chen, *J. Colloid Interf. Sci.,* 2013, **397**, 137–143.
14. L. Yu, H. Liu, C. Liu, H. Lan and J. Qu, *Part. Part. Syst. Charact.,* 2016, **33**, 323–331.